Optimisation of double resonance optically pumped Rb atomic clocks using a reconfigurable physics package testbed

Nitika Gupta, Hugh Klein, Guilong Huang, Rabia Ince, Nyra Ashraf, Ulas Gokay, Laurence Nicholls and Mohsin Haji
Time and Frequency Dept., National Physical Laboratory, Hampton Road, Teddington, United Kingdom, TW11 0LW.
nitika.gupta@npl.co.uk

***Abstract*—The optimisation of a double resonance optically pumped (DROP) rubidium (Rb) atomic clock using a reconfigurable physics package testbed is reported. The testbed can incorporate numerous sizes and variations of the following components: optical sources, Rb vapour cells and microwave cavities. DROP measurements were carried out for a range of different optical powers and temperatures. For one of the Rb vapour cells studied, near optimum physics package conditions were achieved at 75 °C with a DROP signal contrast of 8.7%, a linewidth of 2.3 kHz, and an optical power of 25 µW. In addition, the extent of helium permeation through the walls of a commercial Rb integrated cell was determined by immersing a Rb atomic clock in pure helium at atmospheric pressure and monitoring the drift of the 10 MHz output. A fractional drift rate in normal air (with 5 ppm helium) was determined to be nearly 10^{-11}/month.**

Keywords— Atomic clock, double resonance optical pumping (DROP)

I. INTRODUCTION

Rubidium atomic frequency standards (RAFS) are widely deployed as holdover atomic clocks in a variety of applications such as GNSS, telecommunications and other areas of critical national infrastructure [1-3]. These frequency standards must be optimised to ensure the best stability, since this is crucial for holdover. These holdover clocks contain a physics package which is made up of a Rb vapour cell located coaxially within a microwave cavity. Other components include: an optical source (either lamp or laser), an optional integrated filter cell, heaters, magnetic shields, and magnetic field coils.

In order to optimise the clock, it is essential to understand the effect of temperature fluctuations and its sensitivities to various components of the physics package. Previous research shows that the stability of a compact clock depends predominantly on linewidth, SNR and the contrast of the optical transition [3-5]. The best RAFS have demonstrated an instability of 3 x10^{-15} per day [6] which is approaching H-maser performance levels. Nevertheless, there is still scope for optimising the cavity and vapour cells for reduced size, weight and power (SWaP) leading to lower-cost devices.

This paper presents a robust testbed which was developed at the National Physical Laboratory (NPL), UK to carry out optical spectroscopy and double resonance optically pumped (DROP) in Rb vapour cells for atomic clock applications. Studies were carried out in a reconfigurable physics package so that the clock component parameters could be adjusted. Cells containing helium (He) display a pressure dependent microwave shift; the absolute frequency offset and aging is dependent on the He-permeation rate through the cell's glass walls [7].

Funding from InnovateUK is acknowledged together with advice from collaborators and colleagues.

A separate experiment investigating the extent of this helium permeation was carried out by immersing a commercial compact Rb clock in to pure helium for several days.

II. RECONFIGURABLE TESTBED DESIGN

The reconfigurable testbed is composed of three main components, as shown in figure 1 comprising:

A. Optical Light Source

The testbed allows switching the optical source from broad spectrum lamps to narrow linewidth lasers. A commercial 795 nm extended cavity diode laser (ECDL) was used as the baseline to characterise the Rb vapour cells. Rb vapour cells contain both Rb atoms and buffer gas whereas Rb reference cell contain only Rb atoms. The lasers were locked to the 795 nm absorption line corresponding to the transition ^{87}Rb $5^2S_{1/2} \rightarrow 5^2P_{1/2}$ in rubidium. The latter was obtained from a Rb reference cell.

B. Physics package

Physics package is considered as main part of a miniature atomic clock that decides the clock's performance. The design of the physics package and its components are discussed in the sub section 'characterisation of physics package microwave frequency resonance' under the section 'analysis and discussion'.

C. Signal detection and servo loop

Light through the cell is detected using a photodetector which is then amplified using a biased transimpedance amplifier. This signal goes in through a servo loop. The servo-loop includes a 6.835 GHz microwave synthesiser, lock-in amplifier, integrator and a quartz oscillator that tunes the microwave frequency. The clock stability was measured by locking the quartz oscillator to the atomic reference and comparing its 10 MHz output against a hydrogen maser's 10 MHz signal using a phase noise analyser.

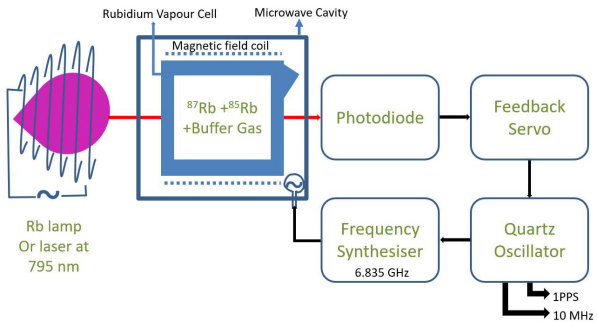

Fig. 1. Schematic of the reconfigurable physics package testbed used to study Rb vapour cells

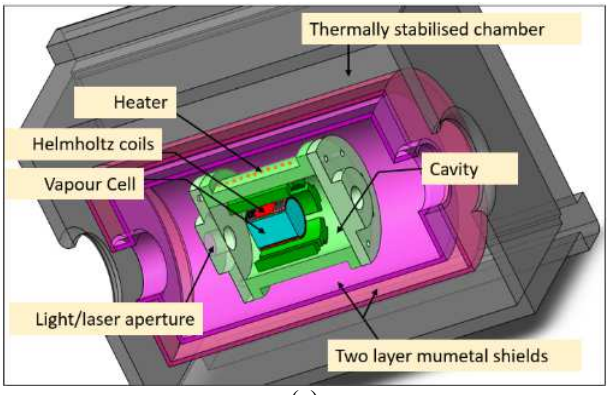

(a)

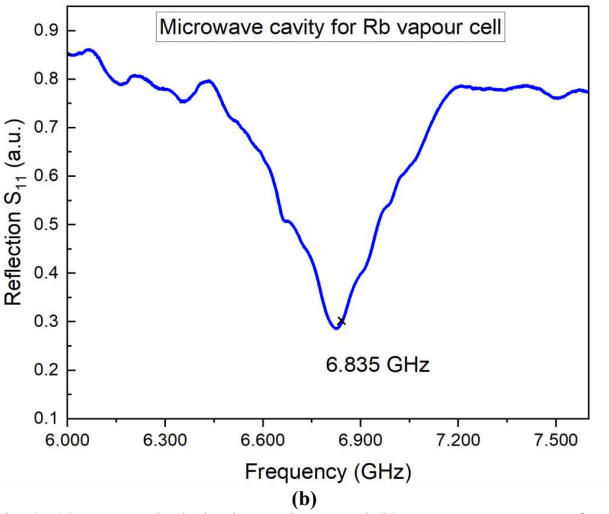

(b)

Fig. 2. (a) NPL testbed physics package, and (b) Frequency response from the microwave cavity

III. Analysis and Discussion

A. *Characterisation of physics package microwave frequency resonance*

The reconfigurable physics package is shown in figure 2(a) and has been designed to accommodate different microwave cavities and Rb vapour cells. The testbed used a magnetron-type cavity (in green) enclosing a Rb vapour cell placed coaxially within the cavity. A cell length of up to 30 mm can be accommodated within the magnetron cavity, with a maximum diameter of 25 mm. For heating the package, a thin high resistance coil (shown in the figure 2(a) as orange dots) is wound across the outside curved surface of the magnetron. Another coil (in red) is wound on the cell itself and generates a magnetic field along the axis of the cavity. The magnetron cavity is enclosed within two mu-metal shields (in purple) to shield it from ambient magnetic fields. The cavity enclosed in the mu-metal shields is thermally insulated using glass wool between the metal chamber and outer mu-metal sheets, shown in grey. This produces a thermally stabilised chamber.

The frequency response of the cavity was measured using a vector network analyser. The microwave frequency S_{11} reflection coefficient response of the cavity is shown in figure 2(b). It was observed before placing the physics package in the testbed.

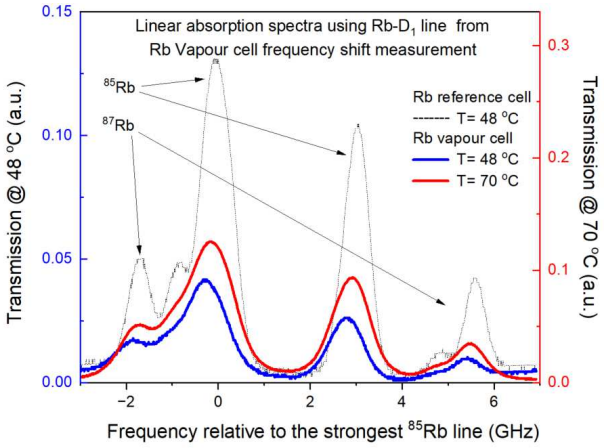

Fig. 3. Linear optical absorption spectra from Rb vapour cell

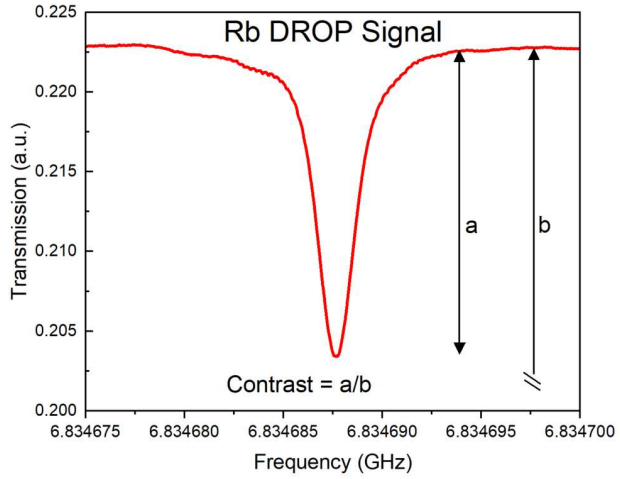

Fig. 4. DROP signal transition $5^2S_{1/2}$ F =1, $m_F = 0 \rightarrow 5^2P_{1/2}$ F =1, $m_F = 0$

The resonance has a linewidth of 330 MHz, with the Rb clock transition frequency centred near to 6.835 GHz.

B. *Optical linear absorption spectroscopy*

Optical linear absorption spectroscopy was performed using an ECDL laser scanned across a region centred on 795 nm. The spectra of the pure Rb reference cell and Rb vapour cell are shown in figure 3.

The frequency spectrum consists of both isotypes: Rb-87 and Rb-85 and shows their corresponding absorption features. The spectrum in black is from the Rb reference cell, the blue and red spectra are of the Rb vapour cell, measured at two temperatures, 48 °C and 70 °C, respectively. Buffer gas in the cell causes the Rb optical spectrum to shift due to collisional interactions between the buffer gas and Rb atoms [8,9]. As the temperature of the cell increases, the pressure inside the cell changes, causing the buffer gas related frequency shift to change.

C. *Double resonance optical pumping (DROP)*

DROP measurements were performed with the Rb vapour cell in a temperature-controlled physics package, shown in figure 4. The laser was locked to the ^{87}Rb $5^2S_{1/2}$ F=1→ $5^2P_{1/2}$ F=2 optical transition, indicated on the rightmost feature of the optical spectra in figure 3.

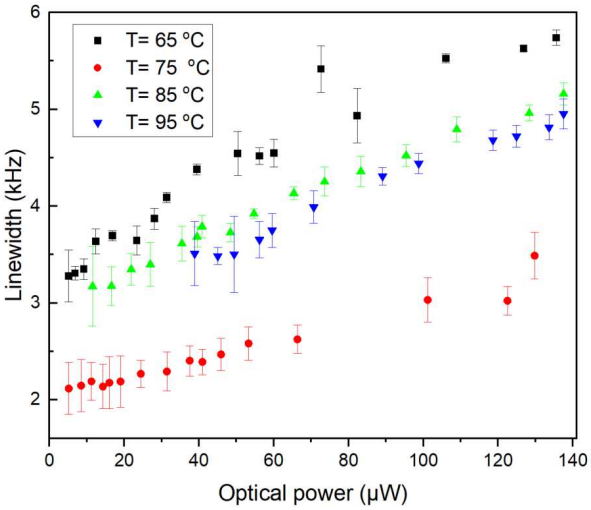

(a)

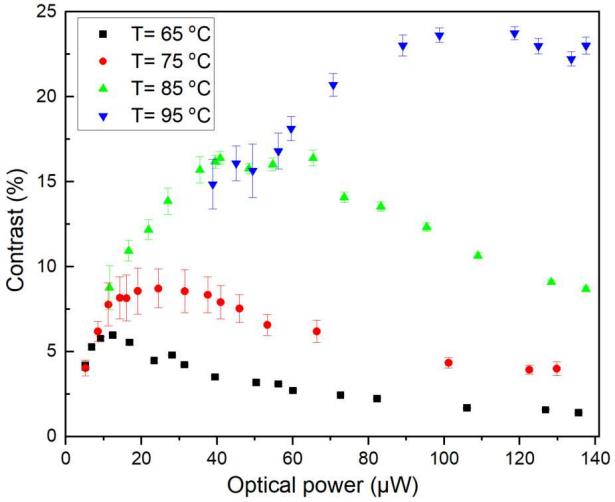

(b)

Fig. 5. Dependence of optical power on DROP (a) linewidth (b) signal contrast

The DROP signal exhibits a resonance which was driven by the application of microwaves. The feature is the $5^2S_{1/2}$ F =1, $m_F = 0 \rightarrow 5^2P_{1/2}$ F =2, $m_F = 0$ "clock transition" which is linearly independent of magnetic field. The signal has a linewidth of 2.3 kHz and a contrast of 8.7 %. When dithering the microwave synthesiser, a lock-in amplifier was used to generate an error signal (not shown). This error signal was used as the input to an integrator to keep the microwaves locked to the clock transition.

Figure 5 shows the measured DROP signal linewidth and contrast variation as a function of optical power at four different temperatures from 65 ºC to 95 ºC.

D. Helium permeation

The extent of helium permeation in commercial rubidium microwave clocks, with an integrated cell, was studied by immersion in one atmosphere of pure helium for a few days. A 10 MHz output was monitored throughout this period and the experiment was repeated three times. The average drift of the 10 MHz signal was $7.6 \pm 0.8 \times 10^{-6}$ Hz/sec.

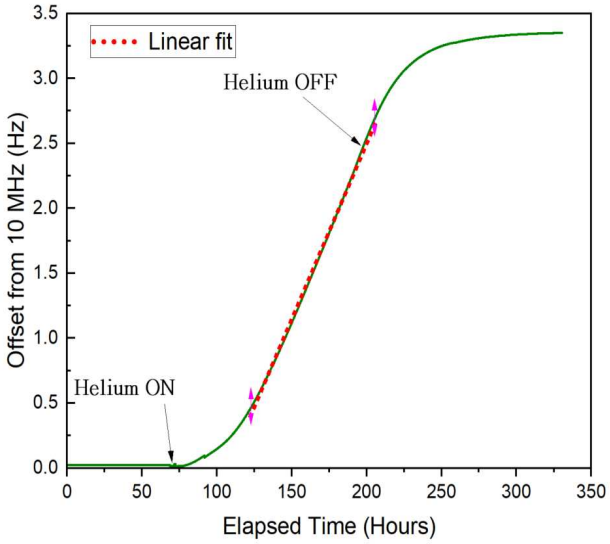

Fig. 6. Frequency shift due to helium permeation in a commercial atomic clock

A second identical clock was monitored at the same time and exhibited similar shift rates. The Earth's atmosphere contains 5 ppm of helium, we can therefore estimate an equivalent drift of $3.8 \pm 0.4 \times 10^{-11}$ Hz/sec, or a fractional drift of $9.8 \pm 1.0 \times 10^{-12}$/month, in normal air. These results have shown that helium permeation into the cell under normal operation will contribute to the overall ageing of these clocks. Careful consideration of glass type and glass coatings is required to help minimise helium permeation.

IV. CONCLUSION

This paper reports recent measurements on Rb vapour cells in an in-house reconfigurable physics package testbed. The testbed can accommodate a variety of optical sources, different cavity designs and vapour cells of varying dimensions. The ability to easily switch clock components is useful in determining the optimum conditions for enhanced signal linewidth and contrast. The thermally controlled physics package shows a DROP signal of 2.3 kHz linewidth and 8.7% contrast measured at 75 ºC. Identifying the optimum operating conditions helps reduce instability in the clock performance. The extent of helium permeation through the walls of a commercial Rb integrated cell was investigated and a fractional drift rate in normal air was determined to be nearly 10^{-11}/month.

Rb microwave atomic clocks continue to be one of the most widely used holdover clocks. A better understanding of optimum physics package parameters and operating conditions will lead to improved performance in commercial Rb clocks. This will allow manufacturers to target better SWaP, lower component costs, and simplify device design.

REFERENCES

[1] W. J. Riley, "A History of the Rubidium Frequency Standard" UFFC-S Hist., vol. July, pp. 1-34, 2019.

[2] J. Camparo, "The rubidium atomic clock and basic research," Phys. Today, vol. 60, no. 11, pp. 33–39, 2007.

[3] M. Violetti, F. Merli, J-F. Zürcher, A. K. Skrivervik, M. Pellaton, C. Affolderbach, G. Mileti, "New miniaturized microwave cavity for Rubidium atomic clocks," Proc. IEEE Sensors, pp. 315–318, 2012.

[4] Q. Hao, W. Xue, F. Xu, K. Wang, P. Yun, and S. Zhang, “Efforts towards a low-temperature-sensitive physics package for vapor cell atomic clocks,” Satell. Navig., vol. 1, no. 1, pp. 1–6, 2020.

[5] M. V. Romalis, E. Miron, and G. D. Cates, “ Pressure broadening of Rb D_1 and D_2 lines by ^{3}He, ^{4}He, N_2, and Xe: Line cores and near wings ,” Phys. Rev. A, vol. 56, no. 6, pp. 4569–4578, 1997.

[6] G. Mei, D. Zhong, S. An, F. Zhao, F. Qi, F. Wang, G. Ming, W. Li, P. Wang, “Main features of space rubidium atomic frequency standard for BeiDou satellites,” 2016 Eur. Freq. Time Forum, EFTF 2016, pp. 1–4, 2016.

[7] J. Camparo and C. Klimcak, “Influence of the atmosphere on a rubidium clock’s frequency aging,” 39th Annu. Precise Time Time Interval Syst. Appl. Meet. 2007, pp. 317–322, 2007.

[8] K. A. Kluttz, T. D. Averett, and B. A. Wolin, “Pressure broadening and frequency shift of the D_1 and D_2 lines of Rb and K in the presence of ^{3}He and N_2,” Phys. Rev. A - At. Mol. Opt. Phys., vol. 87, no. 3, pp. 3–7, 2013.

[9] O. Kozlova, S. Guérandel, and E. De Clercq, “Temperature and pressure shift of the Cs clock transition in the presence of buffer gases: Ne, N_2, Ar,” Phys. Rev. A - At. Mol. Opt. Phys., vol. 83, no. 6, pp. 1–9, 2011.